THE AMERICAN SOCIETY OF MECHANICAL ENGINEERS
345 E. 47th St., New York, N.Y. 10017

98-GT-588

ROLE OF BLADE PASSAGE FLOW STRUCTURES IN AXIAL COMPRESSOR ROTATING STALL INCEPTION

Donald A. Hoying
Air Force Research Laboratory
Wright-Patterson Air Force Base
Dayton, Ohio

Choon S. Tan, Huu Duc Vo
Gas Turbine Laboratory
Massachusetts Institute of Technology
Cambridge, Massachusetts

Edward M. Greitzer*
United Technologies Research Center
East Hartford, Connecticut

ABSTRACT

The influence of three-dimensional flow structures within a compressor blade passage has been examined computationally to determine their role in rotating stall inception. The computations displayed a short length-scale (or spike) type of stall inception similar to that seen in experiments; to the authors' knowledge this is the first time such a feature has been simulated. A central feature observed during the rotating stall inception was the tip clearance vortex moving forward of the blade row leading edge. Vortex kinematic arguments are used to provide a physical explanation of this motion as well as to motivate the conditions for its occurrence. The resulting criterion for this type of stall inception (which appears generic for axial compressors with tip-critical flow fields) depends upon local flow phenomena related to the tip clearance and it is thus concluded that the flow structure within the blade passages must be addressed to explain the stability of an axial compression system which exhibits such short length-scale disturbances.

NOMENCLATURE

C_x	: Axial velocity
M_∞	: Upstream relative incoming flow Mach number
R	: Gas constant
S	: Entropy
U	: Tip blade velocity
γ	: Specific heat ratio
ϕ	: Flow (axial velocity) coefficient, C_x/U
ρ	: Density
E^3	: *Energy Efficient Engine*

*Permanent address: Gas Turbine Laboratory, Massachusetts Institute of Technology

INTRODUCTION AND BACKGROUND

The marked effect of axial compressor tip clearance on stable flow range is a trend which is well documented from an overall performance point of view (Smith, 1970; Koch, 1981; Cumpsty, 1989). In terms of knowledge of the basic mechanisms, however, the phenomenological links connecting tip clearance flow features to the onset of rotating stall (the event that sets the limit on the stable flow range) have by and large not been identified. In particular, on a blade passage scale, there is no accepted qualitative, let alone quantitative, description of the dynamic processes associated with transition from a situation in which the flow has blade-to-blade periodicity (including the embedded tip clearance vortex) to the strong asymmetry which characterizes rotating stall. This paper addresses the connection between tip clearance flow phenomena and rotating stall inception and illustrates the role played by the clearance vortex structure in one of the routes to compressor instability.

The work described here was motivated by the observation that two types of rotating stall inception occur in axial compressors. The first, which is characterized by waves with length-scales on the order of the circumference of the compressor, and propagation speed of one-fourth to one-half of rotor rotation, has been referred to as modal stall inception. A number of investigations have been conducted of this phenomenon (e.g. Haynes, Epstein, and Hendricks, 1994; Tryfonidis et al.,1995), and a main conclusion is that modal development of rotating stall is associated with the growth of small amplitude sinusoidal (in the circumferential coordinate) flow disturbances. Relatively simple models which view the blade passage as a one-dimensional channel (Moore and Greitzer, 1986; Haynes et al., 1994) yield good predictions of the rotational speed, growth rate, and waveform shape of such disturbances. The agreement between experi-

Presented at the International Gas Turbine & Aeroengine Congress & Exhibition
Stockholm, Sweden — June 2–June 5, 1998

ment and model implies that knowledge of the overall blade row loss (or equivalently pressure rise) and turning characteristics suffices in developing a useful analysis of the unsteady fluid dynamic features of the instability process. In this context, the clearance flow structure (clearance vortex) is only important insofar as it affects this overall loss and turning, and it does not appear to be necessary to describe the passage flow on more than this global level to provide a physically meaningful description of instability inception.

There is, however, another, and very different, route to rotating stall, which is characterized by the appearance of disturbances with a dominant length-scale much shorter than the circumference, typically on the order of several blade pitches, as well as a higher propagation speed (70 to 80% of rotor frequency) (Day, 1993). In contrast to modal stall inception, there is currently no mechanistic description of this phenomenon, which has been referred to as short length-scale stall inception or "spikes". Experiments show that this type of rotating stall inception possesses a radial structure (Silkowski, 1995) and that changes in the size of the tip clearance can modify the type of stall inception observed (Day, 1993).

The observations imply (and this paper will confirm) that a different, and more detailed approach is essential to capture the development of such short length-scale stall inception. More specifically, it is necessary to include a description of the tip clearance flow structure within the individual blade passages. In this connection, in view of the pronounced effects which changes in tip clearance have on compressor stability, an important goal of this study is to clarify the link between tip clearance flow and the rotating stall onset. A specific fluid dynamic question, therefore, is what is the role of the tip clearance flow, and the tip clearance vortex, in the stall inception process.

METHODOLOGY AND COMPUTATION/MODELING INTERFACE

Overall Approach and Focus

From the outset it is important to recognize the implications concerning this approach which stem from the observed length-scale and structure of the short length-scale disturbances. Most current approaches to describing rotating stall onset and growth employ a description in which the identities of the individual blades are lost and a particular blade row is replaced by a continuous distribution of body forces or by actuator disks which embody a similar physical concept. Such an approximation relies on the circumferential length-scale of the disturbances of interest being much larger than the blade spacing. In these treatments the blade passage is viewed essentially on a control volume basis, and they cannot thus describe events occurring within the control volume. Anticipating somewhat the results to be shown, however, it can be expected that this information is needed to define the inception mechanism associated with short wave length disturbances. There is thus a requirement to describe, at an appropriate level, those aspects of blade passage flow structure relevant to rotating stall onset.

Another facet of the approach stems from the fact that current computational capabilities are insufficient to allow a full unsteady computation of rotating stall with an arbitrary level of detail. The present method, and this cannot be too strongly emphasized, was thus developed with a specific focus on the rotating stall problem. Although the development of a new computational approach is discussed, this is only a secondary counterpoint to the main theme of the paper, which is to provide insight into the physical processes of interest.

The development of an appropriate description of this problem has involved choices at a number of levels, ranging from selection of computational scheme to basic conceptual issues of what should be modeled and what should be computed directly. As an example of the latter, consider the flow through the tip clearance. A number of studies have shown that for compressors the tip leakage is very nearly a pressure driven cross-flow, that viscous effects in the tip clearance gap have little effect on the overall pattern of the leakage, and that methods which represent the tip clearance flow in a rudimentary manner appear to capture much of the basic behavior (Storer and Cumpsty, 1991; Adamczyk et. al, 1993). Based on this information, it would be expected that one could decrease the computational resources required by treating the tip clearance as an inviscid region, with little or no effect on the overall objective of the study, and this was the approach taken.

Explicitly, what is sought is more nearly conceptual than numerical. We wish to obtain physical conclusions which are firmly grounded in the demonstration that the method captures the experimentally observed trends, i.e., that the overall behavior, from both steady and unsteady view points, is consistent with experiment. Metrics for the calculation thus include not only steady state behavior (rotor loss dependence having approximately the same shape as experiments) but also unsteady flow features (computed short wave length disturbance with the same length-scale, propagation speed, radial profile, and growth rate as seen in the measurements). In summary there have been a number of deliberate, and end objective driven, decisions taken about where to put the 'interface' between computation and modeling to best attack this computationally intensive problem.

Specific Issues to be Resolved

The physical features that need to be addressed are as follows: (i) There are multiple blade passages involved in a rotating stall cell and thus a potentially larger range of length-scales to be captured by the numerical method than in the computation of flow in periodic blade passages (He (1997) has discussed unsteady 3-D Navier-Stokes simulation of 10 blade passages of NASA rotor 67.) (ii) The phenomenon is wave-like and the large range in length-scales therefore implies a similar range of time-scales. The wave behavior of this unsteady flow needs to be appropriately re-

solved. (iii) The compressor operating regime is off-design and the viscous effects which give rise to separated flow must be included. A related consideration was the division of the flow into regions of viscous and inviscid flow, as well as the amount of resolution needed for the boundary layers. (iv) As mentioned previously, the three-dimensional flow structure associated with the tip clearance must be included.

The most challenging aspect of the problem is dealing with the range of length and time-scales. A numerical integration method for dealing with this aspect of the simulation, known as a Dispersion Relation Preserving scheme, has been developed by Tam and Webb (1993). This method was created for wave propagation problems in which accurate representation of dissipative and dispersive behavior is critical. The method is a finite difference approach using an explicit time integration scheme, which possesses a factor of two improvement (in the range of wave lengths that can be propagated accurately) compared to a four-stage Runge-Kutta scheme.

To include the effects of viscosity, a k-ϵ turbulence model was incorporated with a Navier Stokes solver to compute the flow within the compressor. Inclusion of viscous effects near the blades is clearly necessary, but away from the blades viscosity plays little role. The viscous procedure was thus only applied in the near-blade region (sized to include the boundary layers), and outside of this region Euler equations were used.

The most important aspects of the upstream and downstream flow fields in this problem are the pressure and velocity relationships. These can be well described on the basis of an inviscid flow. Put another way, the details of wake mixing in the downstream region would not be expected to have a dominant effect on the unsteady blade row behavior, and it is the latter which is critical in this problem. An Euler representation was therefore also used upstream and downstream of the blades. To further reduce the computational resources required, three-dimensional non-reflecting boundary conditions were developed, allowing shortening of the computational domain by over a factor of two.

The aspects of the code development presented here serve to illustrate how the features of the rotating stall problem have been utilized to guide the balance between modeling and detailed numerics. Detailed description of the development and validation of the code, including comparison with cascade data, is given by Hoying (1996).

FEATURES OF THE NUMERICAL EXPERIMENT

The computational investigation was based on the low speed version of the E^3 compressor (Wisler, 1981), which had been experimentally observed to exhibit the short length-scale type of stall inception (Silkowski,1995; Park, 1994). This compressor has a set of inlet guide vanes followed by four geometrically identical stages with a hub-to-tip radius ratio of 0.85. The rotors have a blade aspect ratio of 1.2 (compared to 1.34 for the stators) and a maximum tip Mach number of 0.2. In the experiments cited, stall inception location was in the first stage rotor with the strongest indications near the tip. Thus, although the actual compressor consisted of four stages, because the initial development of rotating stall was confined to the first rotor in the experiment, the single blade row geometry could be used to analyze the initial phase of the rotating stall development. The computational domain is a portion of the first rotor consisting of eight blades out of the 54 blades present. The number of eight compressor blades was selected based on (two-dimensional) numerical experiments with the same geometry, which showed that eight blades were capable of also exhibiting a modal stall inception (Hoying, 1996). It is important to have the capability for exhibiting both types of stall inception so as not to prejudice the results.

With eight blades, if one wishes to preserve the three-dimensional shape of the blade, only a fraction of the circumference can be included. The maximum wave length of any non-axisymmetric disturbance is thus limited to eight blade spacings, rather than to the full circumference. The hypothesis put forward, however, is that the short wave length type of stall inception is a local phenomenon, so that beyond a threshold number of blades, the actual fraction of the circumference included should not be critical. With eight blades, the length of time over which periodicity is imposed will not be the same as the amount of time for a revolution of the actual rotor. To keep the distinction clear in what follows, the time it takes for the eight blades to traverse the computational domain once will be referred to as a *period* rather than a *revolution*.

The steps in the overall computational procedure involved computing the "axisymmetric" performance using a single periodic blade passage calculation with no throttle transient, followed by the multiple blade passage computation with a throttle-induced transient to allow for the presence of asymmetric flow. The single passage computation was performed to define the flow regimes of interest as well as to permit a comparison between axisymmetric and non-axisymmetric flow fields. In the multiple blade passage calculation, no asymmetries were imposed as the small deviations arising from numerical precision errors were sufficient to induce non-axisymmetric flow during the multiple blade computations. The details of the stalling process were then analyzed much as experimental information had been previously.

Clearances of 1.3% and 3.0% (of chord) corresponding to those examined experimentally were numerically simulated. In the computations, as in the experiment, the results were qualitatively similar between the small and large clearances. Only the results from the 3.0% case will be presented here for clarity. The blade Mach number in the computations (0.2) and in the experiments were much less than unity ($\sim$ 0.2) so the flow could be considered incompressible for both. Before the compressor was throttled to stall, a steady state solution was obtained near the peak of the characteristic given by the single blade passage computation. The compressor mass flow was then reduced by a throttle transient from this steady solution, at a flow coefficient of 0.335,

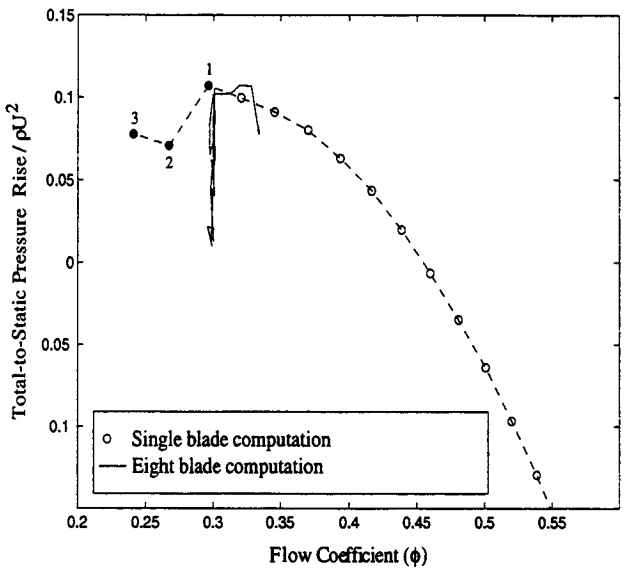

Figure 1: **Pressure rise characteristic for the E^3 rotor. Point 1 is the stall point in the single blade passage calculation. Points 2 and 3 are the corresponding results with throttle closed beyond stall. The speedline for the eight blade calculation shows temporal fluctuations in pressure rise at stall.**

to a value of 0.300 in 3 periods, with conditions then held at a constant throttle setting while the rotating stall pattern developed. The large throttle change was made to avoid the long computational time required from performing multiple small throttle changes.

Figure 1 shows rotor pressure rise versus flow coefficient (based on a stream thrust average) for both the steady-state single blade configuration and the transient eight blade computation (following a single blade passage). The numbered points shown correspond to axisymmetric flow behavior at and past stall, as obtained from the single blade passage calculation. The substantial difference in the behavior near point 1 which represent the quantitatively different flow fields between the blade-to-blade periodic solution and the eight blade calculation is evident. Prior to stall, the difference lies in the unsteadiness in the multi-blade passage calculation, where pressure fluctuations are accentuated by the axially longer flow domain (higher fluid inertia) required in the computation. Since the points on the multi-blade passage speedline represent snapshots in time, they include both the high and low points of the fluctuations and are thus above and below the mean speedline from the single-blade passage calculation. The stall point, characterized by a discontinuity in the slope of the single blade passage speedline and by a temporal fluctuation in pressure rise (at approximately constant overall flow coefficient) of the multi-blade passage speedline, matches in both calculations. However, flow behavior at and after stall is substantially different as explained later.

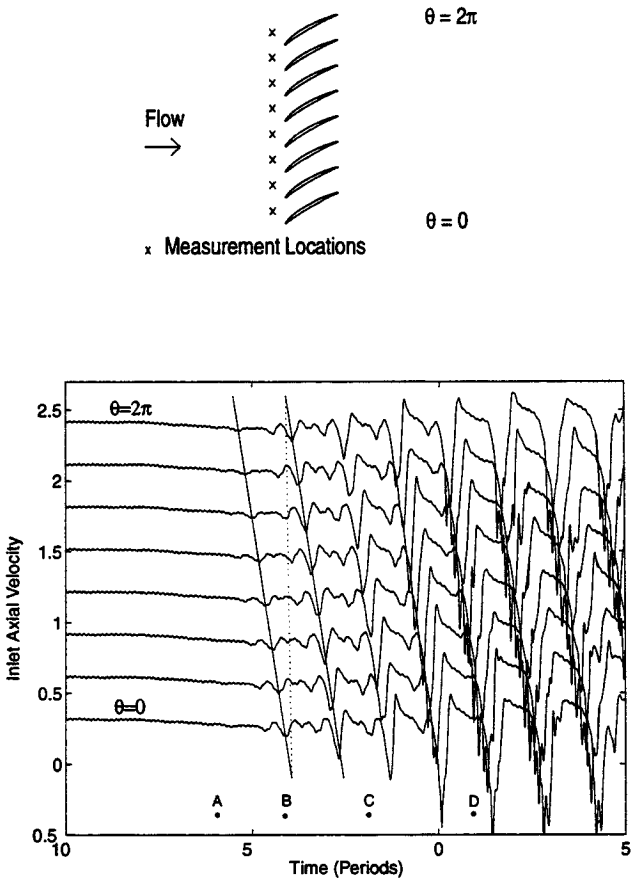

Figure 2: **Traces of the inlet axial velocity at 10% radial immersion from the outer case for the E^3 rotor during a transient to stall. Points A, B, C and D represent four different times in the stall development process.**

CHARACTERIZATION OF THREE-DIMENSIONAL STALL INCEPTION

In analyzing the computations, the primary focus was on characterizing the flow features which participate in the development of short length-scale stall. We can divide discussion of the results into the following steps: (i) demonstrate that the computed stall inception is the same physical event as that observed in experiment, (ii) identify the flow structures which are important in defining this process, (iii) analyze the development of these structures to provide a physical description of the inception of rotating stall.

Direct indication of the evolution of the rotating stall disturbance can be seen from the velocity distribution ahead of the compressor. Figure 2 shows traces of axial velocity parameter ($C_x/U = \phi$) versus time, in units of rotor *periods*, at eight evenly spaced circumferential locations across the eight blades, at 10% radial immersion from the outer case, 1/4 chord ahead of the rotor. An offset has been added to all of the traces except the bottom one to allow them to be viewed together. The traces show the rapid growth of a large amplitude short wave length disturbance in the time

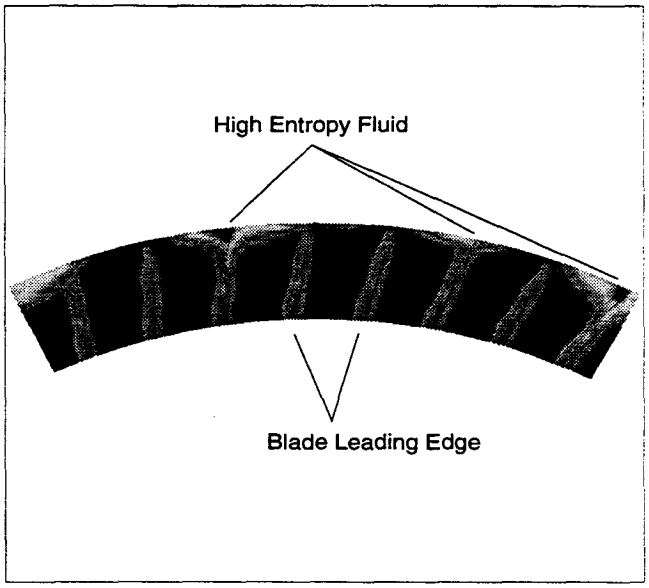

Figure 3: **Entropy contour at the leading edge of the E^3 compressor (Time = -4.1, S =-0.15 to 2.24).**

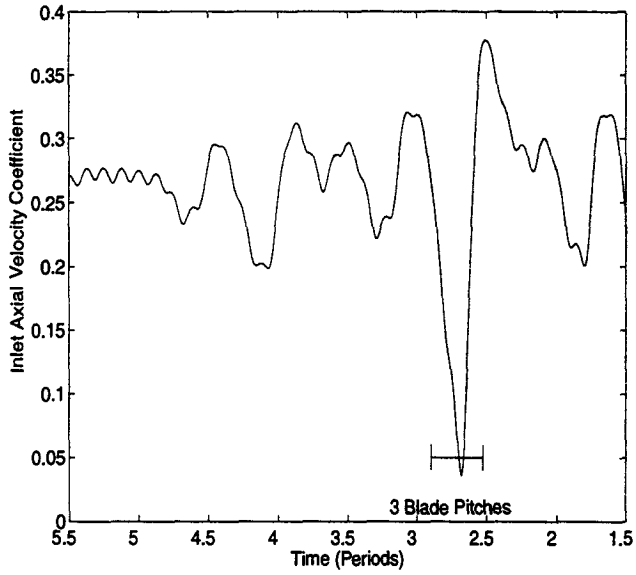

Figure 4: **Trace of the inlet axial velocity from computations for the E^3 rotor at 10% immersion during transient to stall. (Origin of time scale is arbitrary).**

interval from time = -5.34 periods to time = 0 and the two straight lines indicate the disturbance propagation speed. Points A, B, C and D represents four time samples during the growth of the disturbance. The corresponding flow fields are plotted and discussed later in Figures 7 through 10. The shape and development of these disturbances in the inlet axial velocity are qualitatively the same as the disturbances measured by Day (1993).

Two important features of this evolving flow field are illustrated in Figure 3, which shows entropy contours on the leading edge plane of the compressor, at time = -4.1; the scale goes from -0.15 to 2.24, with entropy nondimensionalized by $\frac{1}{2}\gamma M_\infty^2 R$. Thus, an entropy increase of one unit corresponds to a loss of one relative (to the rotor) dynamic head. First is the presence of flow spilling forward of the rotor blade locally, evidenced by the high entropy (maximum $\Delta S = 2.39$) fluid in the blade passage at the leading edge. Second is that the reversed flow region is confined to the tip of the compressor. These features imply that the stall is associated with the spilling forward of the tip clearance flow.

The defining characteristics of the short wave length disturbances are small circumferential extent, high rate of rotation, high growth rate, and localization near the tip (Day, 1993; Silkowski 1995). The position of the disturbance at the tip of the blades has already been demonstrated in Figure 3. To compare the size and shape of the disturbance, the upstream velocity near the tip is shown in Figures 4 and 5 for the computations and for the experiment (Silkowski, 1995) respectively. The figures show local axial velocity coefficient versus time. Both the numerical and the computational results show a disturbance approximately three blade pitches

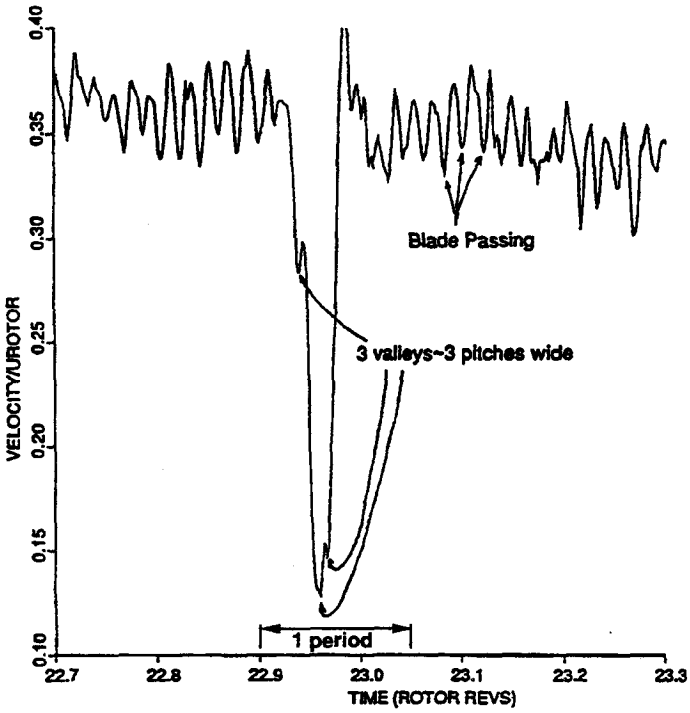

Figure 5: **Trace of the inlet axial velocity stall disturbance for the E^3 compressor tested by Silkowski (1995) at 20% immersion. (Origin of time scale is arbitrary. Total time scale is four periods, the same as that of figure 4).**

wide, although the numerical results indicate several subsidiary disturbances rather than a single spike. Other experiments, however, have shown the development of more than one short length-scale stall cell (Day, 1993), and this difference in the number of stall cells is therefore not considered a key item in the comparisons. The shape of the disturbances shown in Figures 4 and 5 are similar, and the computed rotational speed of the disturbance (70% of rotor speed) also matches the experimental result. One point that should be mentioned is that because the numerical computation does not represent the full compression system used in the experimental investigation, comparison must be done for times when the stalling disturbance is relatively small in axial extent. As the disturbance extent grows, the effect of other blade rows on the disturbance in the rotor will become stronger.

We can also compare the early growth rate of the disturbance. The data of Silkowski (1995) show that the axial velocity disturbance takes roughly one rotor revolution to grow from small amplitude to the value shown in the computed results of Figure 4. In the computation, the corresponding growth takes roughly four periods, which corresponds to 0.6 rotor revolutions, which is on the order of but smaller than the experimental value. On the basis of disturbance shape, radial location, propagation speed, and growth rate, the computations do reproduce the key features of the *initial stages* of the stall inception development observed in experiments. We emphasize that this isolated rotor calculation would not reflect the development of the instability in the multi-stage environment in the long-time limit.

DESCRIPTION OF SHORT LENGTH-SCALE STALLING PROCESS

Using the results, we can now examine the stalling process in more depth. We observed that the motion of the tip clearance vortex was a prominent feature during the development of the stall inception process. It was found that at the operating condition where asymmetry began to develop, the tip clearance vortex trajectory was located at the leading edge cascade plane, i.e., was perpendicular to the axial direction. As rotating stall developed, the vortex moved upstream of the compressor and approximately formed the forward boundary of the reversed flow region of the stall cell.

To view the vortex motion during the development of rotating stall, a sequence of contour plots of the vorticity magnitude at the 92% span radial station are presented in Figures 6-9. (This radial station was used because it gave a clear view of the process.) The different figures correspond to the different times during the stall development process indicated by A, B, C and D in Figure 2.

Just before stall, (Figure 6) the tip clearance vortex stretches from the leading edge of each rotor blade to the leading edge of its nearest neighbor. Figure 7 shows the state 1.8 periods later when non-axisymmetric flow has begun to develop. At this point, as can be seen from the

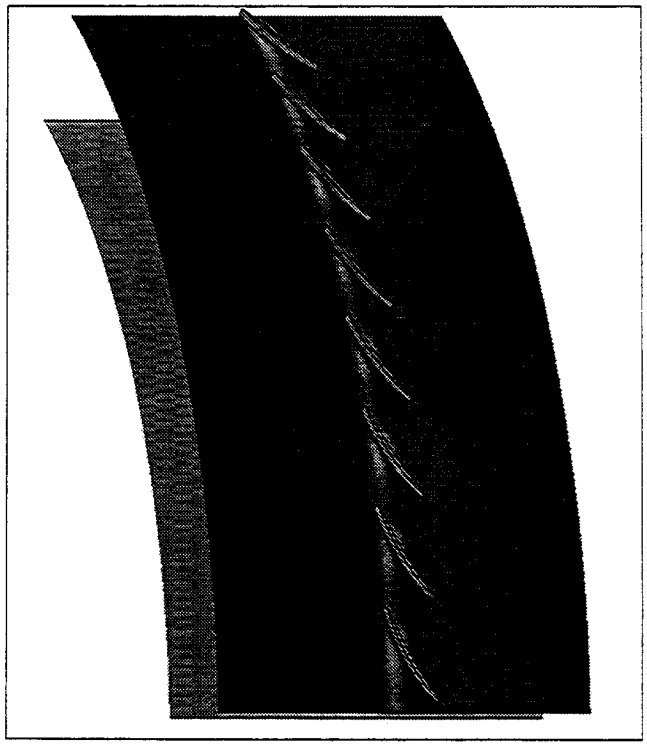

Figure 6: **Vorticity contour at 8% immersion of the E^3 compressor (Time = -5.9, point A in Figure 2).**

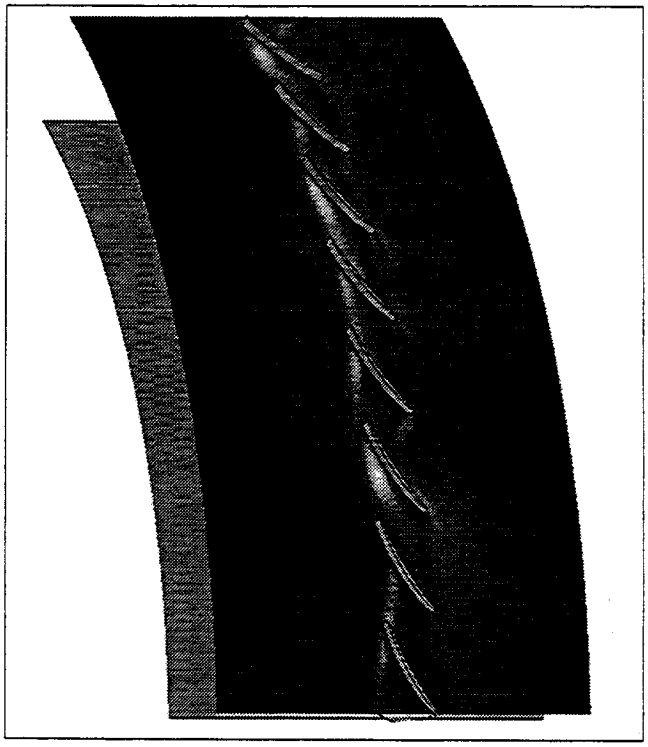

Figure 7: **Vorticity contour at 8% immersion of the E^3 compressor with (Time = -4.1, point B in Figure 2).**

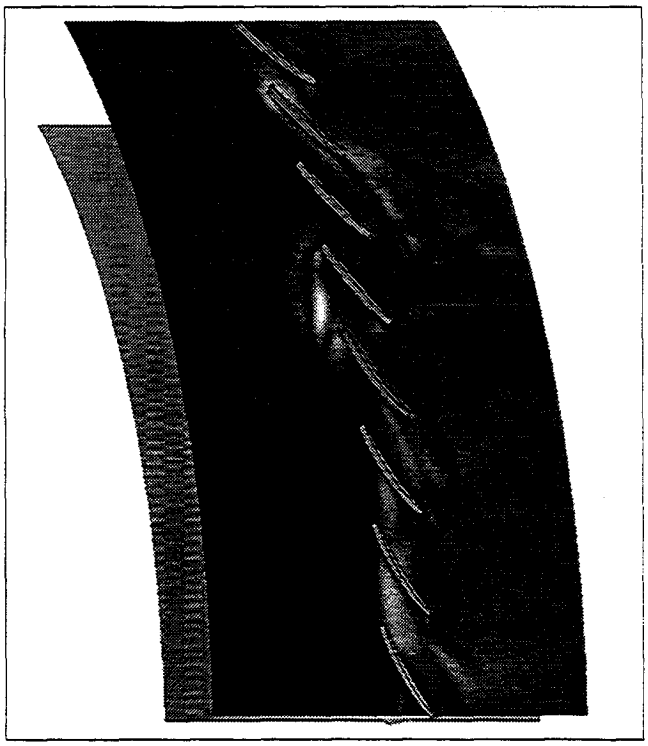

Figure 8: **Vorticity contour at 8% immersion of the E^3 compressor (Time = -1.9, point C in Figure 2).**

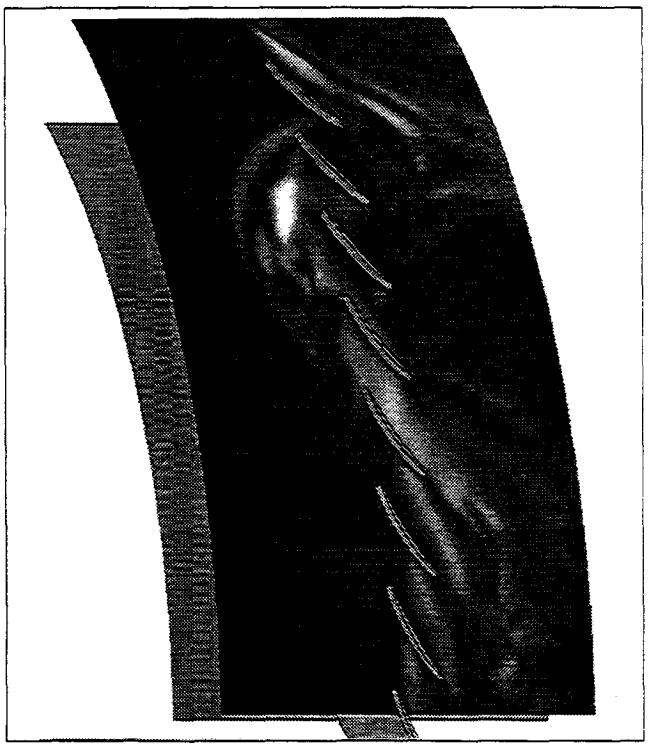

Figure 9: **Vorticity contour at 8% immersion of the E^3 compressor (Time = 1.0, point D in Figure 2).**

corresponding view in Figure 3 which is at the same time, the flow in the lower 3/4 span of the compressor shows no reversal, even though there is reversed flow near the tip. Two to three short length-scale incipient stall disturbances can be seen developing, as evidenced by the presence of the tip clearance vortex forward of the leading edge of the compressor. At a later time, (Time = -1.9) one of these disturbances becomes dominant, as shown in Figure 8, where the clearance vortex is evident at the leading edge of this disturbance. In Figure 9 the dominant disturbance has propagated farther upstream and its width has increased. Later than this, the flow situation is qualitatively similar to Figure 8, but the stall cell grows both axially and circumferentially. Although these pictures are from a single immersion location, corresponding features were evident throughout the outer 10-15% of the span.

The focus has so far been on the motion of tip vortex trajectory. We can also examine quantitatively the two other characteristics of the tip vortex, circulation and blockage, and how they relate to the motion of the tip vortex trajectory during the stall inception process. Blockage can be viewed as the reduction in effective flow area associated with the velocity defect introduced by the low-momentum tip leakage flow forming the vortex (Khalid, 1995). As the throttle is closed toward stall, blockage increases and it is this increase that has been previously linked to rotating stall onset. The connection between tip vortex circulation and stall onset, however, may be more fundamental and it is thus useful to examine the tip vortex circulation and the blockage versus time for a blade passage, shown in Figure 10.

As the nonaxisymmetric flow begins to develop, the circulation of the tip clearance vortex begins an oscillatory motion of increasing amplitude. (Because the data in this plot follows a single blade, the disturbance moves past the blade. If the observer moved with the disturbance it would appear to grow, but not oscillate.) The motion of the vortex is such that when the vortex circulation increases above the pre-stall level, the vortex is forward of the blade row, and when the circulation is less, the vortex is behind the blade row leading edge. The blockage, which has been found to be associated with the vortex core fluid (Adamczyk et al., 1993; Khalid, 1995), at the rotor trailing edge also undergoes a corresponding oscillation. The blockage variation tracks the vortex circulation (and motion), but the blockage lags the vortex strength by approximately 2 blade passing times (0.26 period). This indicates that blockage and tip vortex circulation are linked, although the mechanism responsible for the dynamic behavior of the tip vortex has not yet been resolved.

ROLE OF THE TIP CLEARANCE VORTEX IN SHORT LENGTH-SCALE STALL

Insight into the mechanism of short wavelength stall development can be obtained by considering the behavior of the vortex trajectory. Figure 11 shows the stable trajectories at four different flow coefficients from high flow ($\phi = 0.38$)

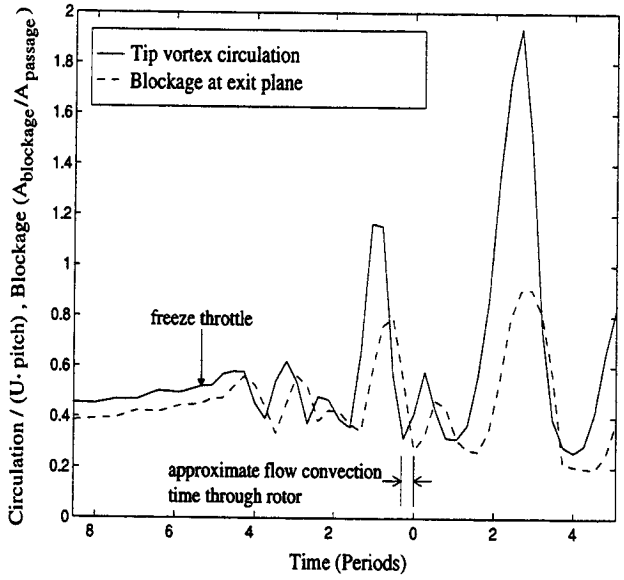

Figure 10: **Tip vortex circulation and trailing edge blockage associated with tip leakage vortex for the E^3 rotor during stall development. An increase in tip vortex circulation corresponds to a movement of the tip vortex trajectory forward of the blade row and vice versa.**

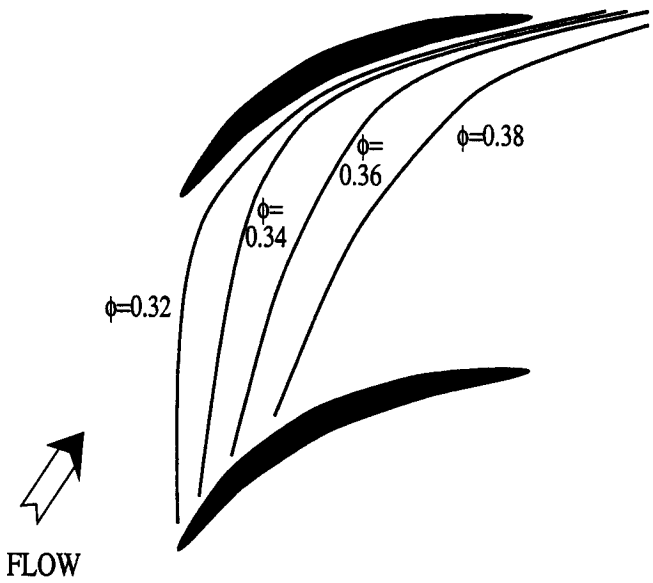

Figure 11: **Trajectories of the tip clearance vortex for the E^3 rotor for different flow coefficients.**

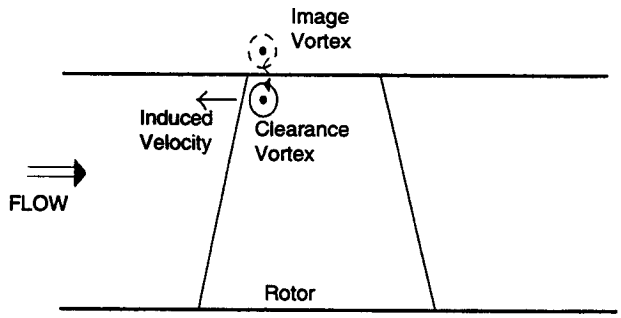

Figure 12: **Velocity induced by image vortex (meridional view).**

to near stall ($\phi = 0.32$). At the higher flow coefficients the vortex trajectory lies further back in the blade passage. As the flow coefficient is reduced the clearance vortex trajectory becomes closer to perpendicular to the axial direction.

The behavior of the vortex equilibrium position can be understood from vortex kinematics, as illustrated in Figure 12 which shows a side view of the vortex in the blade passage along with its image across the casing wall. Because the distance of the vortex from the wall is much less than the span of the vortex along the passage, the local 'self-induced' velocity can be approximated from the local orientation of the vortex, and the velocity field associated with the vortex-boundary configuration can be represented by the vortex and its image. As indicated, the induced velocity of the vortex pair is in the upstream direction.

For a given clearance vortex circulation and mean flow, there will, in general, be an angle for the vortex trajectory at which this self-induced velocity is balanced by the component of the mean flow normal to the vortex. At operating conditions near design, the trajectory will be in an equilibrium position like that shown in Figure 13(a). Consider a displacement of the vortex from this position. If the vortex moves forward, the mean flow vector becomes more closely aligned with the perpendicular to the vortex, resulting in an increased value of velocity component normal to the vortex. The result is that the vortex tends to be returned to the original position. From these considerations, the position is stable.

As the compressor is throttled towards stall, computational results show that the strength of the clearance vortex increases and the mean flow velocity decreases. As the flow coefficient decreases (Figure 13(b)), the equilibrium vortex trajectory swings closer to perpendicular to the axial direction. A stable equilibrium cannot exist when the vortex trajectory becomes perpendicular to axial because the ability of the flow to respond to perturbations through an increased normal component of the axial velocity is lost; if a small perturbation occurs, there is no corrective action associated with the mean flow component normal to the vortex which will restore equilibrium. (For the case studied here, this

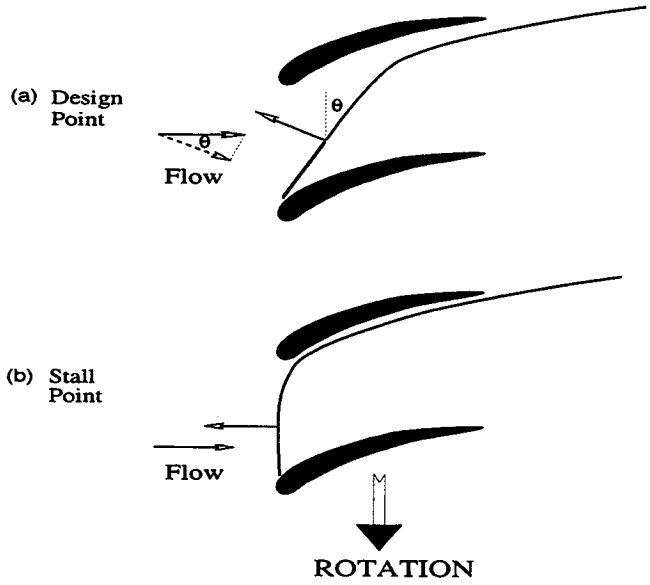

Figure 13: **Trajectory and induced velocity for the tip clearance vortex at different loading conditions. (a) Design point; (b) Stall point.**

point was reached at the peak of the pressure rise characteristic.) The vortex will thus tend to propagate forward of the rotor passage and as noted, the computations show the subsequent growth in displacement out of the blade passage.

Although this description by itself does not explain why the flow breaks down into a nonaxisymmetric short length-scale stall cell, further considerations of the vortex motion are helpful in addressing this aspect. Vortex lines cannot end in the fluid so that when the vortex begins to propagate forward of the compressor, it must do so by bowing forward. The portion of the vortex in the center of the bowed region will remain perpendicular to the flow direction, but the rest of the vortex will be turned away from the main flow direction and will therefore have a locally reduced self-induced upstream velocity. The shape of the upstream propagating vortex will alter as indicated qualitatively in Figure 14, promoting the development of the type of localized disturbance with characteristic length of a blade spacing shown in experiments (Day, 1993).

It can be noted that a description of the entire multi-blade row compression system was not required to demonstrate this unstable flow situation, although the process does not take place in isolation, and at some point the influence of the remainder of the compression system will be felt. The events described are originally local to the tip region of one blade row, and thus not significantly affected by the rest of the compression system during the initial development. The single blade row results should thus apply to the initial development of a short length-scale stall in multi-blade row compressors. For compressors operating near the peak of their characteristic, such disturbances have the potential to

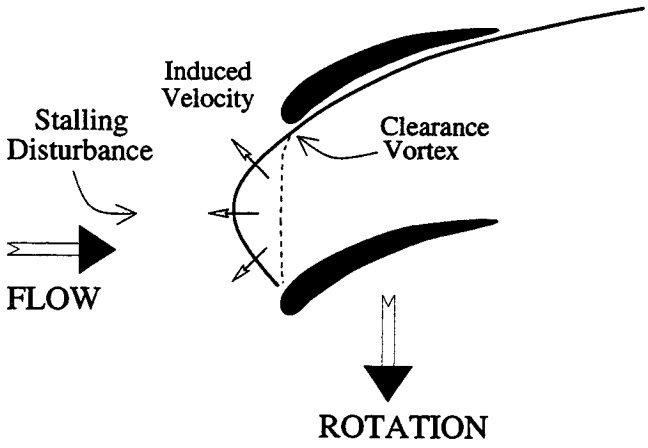

Figure 14: **Development of localized disturbance.**

induce rotating stall to occur in the entire compressor, as described by Gong (1998).

TRANSIENT PERFORMANCE WITH BLADE-TO-BLADE PERIODICITY

We have so far been focusing on the behavior of the tip vortex in a multi-blade passage environment. It would be of interest to assess its behavior in a single (periodic) blade passage situation and determine the usefulness of such a calculation. Single blade passage computations show that once the tip clearance vortex reached the critical position at the leading edge of the blade row at a point on the compressor characteristic represented by point 1 in Figure 1, it would remain there if the throttle were held fixed. If the throttle were closed past this point, (points 2 and 3 in Figure 1), the pressure rise dropped and the tip vortex settled into a new stable position[1] slightly ahead of the blade row with a bowed shape similar to Figure 14. This is different from the multi-blade passage calculation which shows growing fluctuations in pressure rise at the stall point. This behavior is associated with the dynamic motion of the tip vortex alluded to previously. Thus, the single blade calculation can simulate the behavior of the tip vortex up to the point of instability. Beyond this point, the single blade computation cannot simulate the dynamic behavior of the tip vortex because of the inherent assumption that each blade passage is decoupled from the other blade passages.

Two important observations can be derived from the single-blade calculation within its range of validity. First, the stall point closely matches that of the multi-blade calculations (see Figure 1). Second, the negative slope at stall based on the single blade speedline is consistent with past observations of short length-scale stall. (An accurate evalu-

[1]In contrast to the usual pressure exit boundary condition, this computational procedure incorporates a throttle as the exit boundary condition so that a stable solution can be obtained past the stall point.

ation of the slope cannot be made from the multi-blade unsteady computation due to pre-stall oscillations in pressure rise created by the throttle transient.) The above observations suggests that single blade computations may be useful for predicting the stall point for compressor exhibiting short length-scale rotating stall inception, from observation of the tip vortex position.

SUMMARY AND CONCLUSIONS

Computational experiments have been carried out to simulate the short length-scale rotating stall inceptions which have been found to have fundamentally different behavior from long length-scale modal stall. For the former, inception depends essentially upon local flow conditions, whereas for modal stall inception there is a strong interaction with the rest of the compression system.

The short length-scale inception process is linked to the behavior of the blade passage flow field structure, specifically the tip clearance vortex. This is in contrast to the modal stalling case where a description of the flow structures within the blade passages is not required for a useful description of rotating stall inception and development.

A local stall inception criteria for the short length-scale phenomena , namely tip vortex trajectory perpendicular to the axial direction, has been identified for axial compressors. This suggests that for tip-critical compressors (as is the case here) single blade passage calculations, rather than computations of the entire annulus, may be used to predict the conditions at which a short length-scale disturbance can occur.

The origin of this stalling process has also been described in terms of the kinematics of the tip clearance vortex. Stall inception is a result of the motion of the tip clearance vortex moving out (upstream) of the blade passage; this occurs when the vortex trajectory is aligned with the blade leading edge plane which was shown to be an unstable condition. The time evolution of the rotor exit blockage is a consequence of this motion.

The process by which the short length-scale disturbances develop is generic for axial compressors with tip-critical flow fields and a similar breakdown in axisymmetric flow field should be expected in any compressor which experiences a spilling forward of the tip clearance vortex.

While the present set of calculations is for an isolated rotor that is known to exhibit short lenght-scale stall, there is a need to examine the instability behavior (including modal stall inception) of the compressor rotor in a multi-blade row environment.

ACKNOWLEDGMENTS

The authors wish to thank the United States Air Force for funding of this research through the Palace Knight program. Dr. D. C. Rabe was the technical monitor and his interest and support are greatly appreciated. We also acknowledge the many useful discussions with Professors F. E. Marble and N. A. Cumpsty. Partial funding has also been provided by Pratt and Whitney, Mr. R. S. Mazzawy and Dr. 0. P. Sharma, project monitors, and AFOSR Grant no. F49620-96-1-0266, Dr. M. Glauser, technical monitor. Substantial computer support has been provided by the NASA Lewis Research Center and NASA Ames Research Center. These sources of support are gratefully acknowledged.

BIBLIOGRAPHY

Adamczyk, J. J., M. L. Celestina, E. M. Greitzer, 1993, "The Role of Tip Clearance in High-Speed Fan Stall," *ASME Journal of Turbomachinery*, Vol. 115, pp. 28-38.

Camp, T. R., 1995, *Aspects of the Off-Design Performance of Axial Flow Compressors*, PhD Thesis, University of Cambridge.

Cumpsty, N. A., 1989, *Compressor Aerodyanmics*, Longman Scientific & Technical, Essex, England.

Day, I. J., 1993, "Stall Inception in Axial Flow Compressors," *ASME Journal of Turbomachinery*, Vol. 115, pp. 1-9.

Gong, Y., C.S. Tan, K. Gordon and E.M. Greitzer, 1998, "A Computational Model for Short Wave-Length Stall Inception and Development in Multi-Stage Compressor," *Submitted for TurboExpo98*, Stockholm, Sweden.

He, L. and J. O. Ismael, 1997, "Computations of Blade Row Stall Inception in Transonic Flows," *ISABE 1997*, paper number 97-7100, pp. 697-707.

Haynes, J. M., G. J. Hendricks, and A. H. Epstein, 1994, "Active Stabilization of Rotating Stall in a Three-Stage Axial Compressor," *ASME Journal of Turbomachinery*, Vol. 116, pp. 226-239.

Hoying, D. A., 1996, *Blade Passage Flow Structure Effects on Axial Compressor Rotating Stall Inception*, PhD Thesis, Massachusetts Institute of Technology.

Khalid, S. A., 1995, *The Effects of Tip Clearance on Axial Compressor Pressure Rise*, PhD Thesis, Massachusetts Institute of Technology.

Koch, C. C., 1981, "Stalling Pressure Rise Capability of Axial Flow Compressor Stages," *ASME Journal of Engineering for Power*, Vol. 103, pp. 645-656.

Moore, F. K. and E. M. Greitzer, 1986a, "A Theory of Post-Stall Transients in Axial Compression Systems: Part I - Development of Equations," *ASME Journal of Engineering for Gas Turbines and Power*, Vol. 108, pp. 68-76.

Moore, F. K. and E. M. Greitzer, 1986b, "A Theory of Post-

Stall Transients in Axial Compression Systems: Part II - Application," *ASME Journal of Engineering for Gas Turbines and Power*, Vol. 108, pp. 231-239.

Park, H. G., 1994, *Unsteady Disturbance Structures in Axial Flow Compressor Stall Inception*, Master's Thesis, Massachusetts Institute of Technology.

Silkowski, P. D., 1995, *Measurements of Rotor Stalling in a Matched and a Mismatched Multistage Compressor*, GTL Report No. 221, Gas Turbine Laboratory, Massachusetts Institute of Technology.

Smith, L. H. Jr., 1970, *Casing Boundary Layers in Multistage Axial-Flow Compressors*, Flow Research on Blading, ed., L. S. Dzung, Elsevier Pub. Co., Amsterdam.

Storer, J. A. and N. A. Cumpsty, 1991, "Tip Leakage Flows in Axial Compressors," *ASME Journal of Turbomachinery*, Vol. 113, pp. 252-259.

Tam, C. K. W. and J. C. Webb, 1993, "Dispersion-Relation-Preserving Finite Difference Schemes for Computational Acoustics," *Journal of Computational Physics*, Vol 107, pp. 262-281.

Tryfonidis, M., O. Etchevers, J. D. Paduano, G. F. Hendricks, and A. H. Epstein, 1995, "Pre-Stall Behavior of Several High-Speed Compressors," *ASME Journal of Turbomachinery*, Vol. 117, pp. 62-80.

Wisler, D. C., 1981, *Core Compressor Exit Stage Study, Volume IV - Data and Performance Report for the Best Stage Configuration*, NASA CR-165357, NASA Lewis Research Center.